



HAL
open science

Bicelles as a carrier for bioactive compounds in beverages: application to nerolidol, an active sesquiterpene alcohol

Elissa Ephrem, Amal Najjar, Catherine Charcosset, H el ene Greige-Gerges

► To cite this version:

Elissa Ephrem, Amal Najjar, Catherine Charcosset, H el ene Greige-Gerges. Bicelles as a carrier for bioactive compounds in beverages: application to nerolidol, an active sesquiterpene alcohol. *Journal of Food Science and Technology*, 2022, 59 (3), pp.1030-1039. 10.1007/s13197-021-05107-3 . hal-03782986

HAL Id: hal-03782986

<https://hal.science/hal-03782986>

Submitted on 21 Sep 2022

HAL is a multi-disciplinary open access archive for the deposit and dissemination of scientific research documents, whether they are published or not. The documents may come from teaching and research institutions in France or abroad, or from public or private research centers.

L'archive ouverte pluridisciplinaire **HAL**, est destin ee au d ep ot et  a la diffusion de documents scientifiques de niveau recherche, publi es ou non,  emanant des  tablissements d'enseignement et de recherche fran ais ou  trangers, des laboratoires publics ou priv es.

1

2 **Bicelles as a carrier for bioactive compounds in beverages: application to**
3 **nerolidol, an active sesquiterpene alcohol**

4

5 Elissa Ephrem^{1,2}, Amal Najjar¹, Catherine Charcosset^{2*}, H el ene Greige-Gerges^{1**}

6 1. Bioactive Molecules Research Laboratory, Faculty of Sciences, Lebanese University,
7 Lebanon.

8 2. Univ Lyon, Universit e Claude Bernard Lyon 1, CNRS, LAGEP UMR 5007, 43 Boulevard
9 du 11 novembre 1918, F-69100, Villeurbanne, France.

10 *Corresponding author: Univ Lyon, Universit e Claude Bernard Lyon 1, CNRS, LAGEP UMR
11 5007, 43 Boulevard du 11 novembre 1918, F-69100, Villeurbanne, France. E-mail address:
12 catherine.charcosset@univ-lyon1.fr

13 **Corresponding author: Faculty of Sciences, Section II, Bioactive Molecules Research
14 Laboratory, Lebanese University, B.P. 90656 Jdaidet El-Matn, Lebanon. E-mail addresses:
15 greigegeorges@yahoo.com, hgreige@ul.edu.lb (H el ene Greige-Gerges)

16

17 **Abstract**

18 Nerolidol is a natural sesquiterpene alcohol with promising but limited application in food and
19 pharmaceutical fields due to several factors including low photostability and low aqueous
20 solubility. Recently, several carriers loading nerolidol were prepared and tested in fresh orange
21 juice. Lipid vesicles loading nerolidol did not exhibit satisfactory organoleptic properties in this

22 beverage. Hence, DMPC/DHPC bicelles were prepared as a new phospholipid-based carrier for
23 nerolidol at different molar ratios. The bicelle suspensions were characterized in terms of
24 homogeneity, particles size, and morphology. The optimal formulation (phospholipid:nerolidol
25 molar ratio 100:1) was selected based on transparent appearance, homogeneity, and particle size
26 (~45 nm). Besides, it showed a high encapsulation efficiency of nerolidol and a high incorporation
27 rate of phospholipids. Transmission electron microscopy analysis demonstrated the formation of
28 bicelles. The bicelles membrane fluidity was assessed by 1,6-diphenyl-1,3,5-hexatriene
29 fluorescence anisotropy and differential scanning calorimetry analysis. The membrane fluidity of
30 bicelles appeared to increase in the presence of nerolidol in a concentration dependent manner. To
31 our knowledge this is the first study dealing with the encapsulation of an essential oil component
32 in bicelles.

33 **Keywords:** bicelles; differential scanning calorimetry; fluorescence anisotropy; membrane
34 fluidity; nerolidol.

35

36 **Highlights**

37 For the first time nerolidol, a sesquiterpene, was efficiently incorporated in bicelles

38 Suspensions of bicelles loading nerolidol were transparent, homogenous, and stable at 4 °C

39 Bicelles presented high encapsulation efficiency and high molar percentage of Ner

40 High incorporation rate of phospholipids was also demonstrated for the optimal formulation

41 Nerolidol increased the fluidity of bicelles in a concentration dependent manner

42

43 **Abbreviations:** DLS: dynamic light scattering; EE: encapsulation efficiency; HPLC: high
44 performance liquid chromatography; IR: incorporation rate; Ner: nerolidol; PDI: polydispersity
45 index; TEM: transmission electron microscopy.

46

47 **1. Introduction**

48 Bicelles are bilayered nanostructures composed of a mixture of long- and short-alkyl chain
49 phospholipids. The long chain phospholipids form the bilayer of the bicelles whereas the short
50 chain phospholipids form the rim (Dürr et al. 2012) (Fig 1). Dimyristoylphosphatidylcholine
51 (DMPC) and dipalmitoylphosphatidylcholine (DPPC) are the most commonly used long chain
52 phospholipids, and dihexanoylphosphatidylcholine (DHPC) is the most used short-chain lipid to
53 prepare bicelles (Visscher et al. 2006). The bicellar system has been extensively employed as a
54 membrane model to study the structure of membrane proteins and their interaction with
55 phospholipids (Dürr et al. 2012). Bicelles are poorly studied for application in aqueous
56 pharmaceutical preparations and the interest in bicelles for skin application as a replacement for
57 liposomes and micelles has recently emerged (Rubio et al. 2010, 2011). Moreover, bicelles have
58 been proposed as a delivery system for hydrophobic drugs such as the anticancer agent doxorubicin
59 (Lin et al. 2016). To our knowledge, the development of bicelles for food application is not studied
60 yet.

61 The bicellar system has a transparent aspect and combines the properties of classic micelles and
62 liposomes. Compared to micelles, the advantages of bicelles are mainly related to the absence of
63 surfactants (Rubio et al. 2010, 2011). They are generally smaller than liposomes and more stable
64 than micelles, thus they may constitute a promising system for the delivery of active molecules in
65 food, beverages, and pharmaceutical preparations enriched in water. Moreover, the use of
66 liposomes in beverages, such as fruit juice, is challenging as they may change the organoleptic
67 properties of the beverage (Marsanasco et al. 2015).

68 Nerolidol (Ner), 3,7,11-trimethyl-1,6,10-dodecatrien-3-ol, is a sesquiterpene alcohol which
69 exhibits various biological and pharmacological activities, including a significant antimicrobial

70 activity against different microorganisms such as *Corynespora cassicola* and *Staphylococcus*
71 *aureus* (Chan et al. 2016). It has been reported that Ner is a photosensitive agent (Chan et al. 2016);
72 however, its chemical and biological stability is not well documented in literature. Moreover, Ner
73 is poorly soluble in water with a log Kow value of 5.68 and a water solubility of 1.538 mg/L at 25
74 °C (Chan et al. 2016); this encouraged its incorporation in carrier systems. Cyclodextrin/nerolidol
75 inclusion complexes (Azzi et al. 2017), conventional liposomes, and drug-in-cyclodextrin-in-
76 liposomes loading Ner were prepared, characterized and evaluated for their antimicrobial effects
77 in fresh orange juice (Azzi et al. 2018a).

78 Cyclodextrins are natural oligosaccharides known for their capacity to encapsulate a large variety
79 of hydrophobic compound. Cyclodextrins are widely used in the food and pharmaceutical
80 industries to enhance the physico-chemical stability and aqueous solubility of hydrophobic active
81 agents. Cyclodextrins are easy to process and are appreciated for their diverse properties including
82 prebiotic action (α -cyclodextrin), non-toxicity, resistance to shear forces, and neutrality in terms
83 of taste and odor (Moreira da Silva 2009). However, different authors discussed the limitations of
84 the different forms of cyclodextrins used including a limited water solubility (such as β -
85 cyclodextrin), mass limitations for oral dosage units, sensitivity to acidic conditions, and stability
86 of cyclodextrin/guest inclusion complex (Miranda et al. 2011; Chen et al. 2014). Liposomes are
87 microscopic spherical lipid vesicles used for the encapsulation of hydrophilic, lipophilic, and
88 amphiphilic molecules. They are known for their low toxicity, bio-degradability, and bio-
89 compatibility. When applied in water enriched food such as fruit juice, liposome formulations
90 produce milky aspect thus altering the organoleptic property of fruit juices (Ephrem et al. 2019).
91 To the best of our knowledge, this work describes for the first time in literature the development
92 of a DMPC/DHPC bicelles system to carry an essential oil component. Ner was added at different

93 phospholipids to Ner molar ratio, and the optimal formulation was chosen based on the appearance
94 of the formulation, the homogeneity of the suspension, and the size and morphology of the
95 particles. The selected formulation was further characterized in terms of Ner encapsulation
96 efficiency (EE) and molar percentage in bicelles (%Ner), in addition to the incorporation rate of
97 phospholipids (IR) in bicelles. Furthermore, the effect of Ner on the membrane fluidity of bicelles
98 was studied by fluorescence polarization of 1,6-diphenyl-1,3,5-hexatriene (DPH) and differential
99 scanning calorimetry (DSC) analysis.

100 **2. Materials and methods**

101 **2.2. Materials**

102 Dimyristoylphosphatidylcholine (DMPC) and dihexanoylphosphatidylcholine (DHPC) were
103 purchased from Avanti Polar Lipids (USA). Tetrahydrofuran, nerolidol (98%, mixture of *cis*
104 (40%)/*trans* (60%) isomers), and ammonium molybdate were purchased from Sigma-Aldrich
105 (USA). Potassium phosphate monobasic was purchased from Sigma-Aldrich (Mexico). 4-Amino-
106 3-hydroxyl-1-naphthalene sulfonic acid was purchased from Sigma-Aldrich (India). Chloroform
107 and methanol were purchased from Sigma-Aldrich (France). Sulfuric acid, hydrogen peroxide, and
108 thymol (>99%) were purchased from Sigma-Aldrich (Germany). 1,6-Diphenyl-1,3,5-hexatriene
109 (DPH) was purchased from Across Organics (USA).

110 **2.3. Preparation of blank- and nerolidol-loaded bicelles**

111 Blank bicelles were prepared using the long chain phospholipid DMPC and the short chain
112 phospholipid DHPC. The two phospholipids were mixed in chloroform at a DMPC to DHPC molar
113 ratio of 2.0. The chloroform was then evaporated under reduced pressure at 35 °C until the
114 formation of a lipid film. The film was hydrated with 1 mL of ultrapure water (35 °C) to yield a
115 total lipid concentration of 20% (w/v). The obtained suspension was finally subjected to several

116 cycles of freeze-thaw and the size of the particles was monitored after each cycle by DLS analysis.
117 Freeze (0 °C) - thaw (room temperature) cycles were repeated until a transparent solution was
118 obtained.

119 Nerolidol-loaded bicelles were prepared as described for blank bicelles but with the drug dissolved
120 in the chloroform phase. Various phospholipids to Ner molar ratios (100:1, 50:1, 20:1, 10:1, and
121 4:1) were tested for Ner-loaded bicelles formulation.

122 **2.4.Characterization of blank- and nerolidol-loaded bicelles**

123 ***2.4.1. Determination of size, polydispersity index, and zeta potential***

124 The mean size and polydispersity index (PDI) values of the formulations were determined by
125 dynamic light scattering (DLS) using a Malvern Zetasizer nanoSeries (3600, Orsay, France). The
126 PDI is a measure of the width of the molecular weight distribution and thus is an indicator of the
127 suspension homogeneity. The zeta potential value was also obtained with a Malvern Zetasizer
128 nanoSeries (3600, Orsay, France) and it may be related to the stability of the system, as a low zeta
129 potential value may lead to the coagulation of the particles. Prior to each measurement, the sample
130 was diluted with ultrapure water at a temperature of 19 ± 1 °C or 25 ± 1 °C to obtain a count rate
131 between 150 and 300 kilo counts per second.

132 ***2.4.2. Transmission electron microscopy analysis***

133 The morphology of bicelles was determined by transmission electron microscopy (TEM) using
134 Philips CM120 microscope (Eindhoven, The Netherlands) at the “Centre Technologique des
135 Microstructures” (CT μ) at the University of Lyon (Villeurbanne, France). The analyses were
136 performed at an acceleration of 80 kV. An aliquot (10 μ L) of each sample was placed on a carbon-
137 coated copper grid. After 2 min, the liquid excess was removed using a filter paper, to obtain a
138 thin liquid film on the grid. Negative staining was then made using a 1% sodium silicotungstate

139 solution. After 30 s, the excess sodium silicotungstate solution was removed with filter paper. The
140 sample was then left to dry at room temperature.

141 ***2.4.3. Separation of free and encapsulated components***

142

143 Prior to the determination of the encapsulation efficiency and loading rate of Ner and the
144 incorporation rate of phospholipids, free and encapsulated compounds were separated by
145 centrifugation. Therefore, an aliquot of the sample was centrifuged at 14,000 g for 30 min using
146 Vivaspin 500 centrifuge (3000 MWCO, Sartorius, United Kingdom).

147 ***2.4.4. Incorporation of phospholipids***

148

149 Bartlett's method was used to determine the total and free phospholipid concentrations in the
150 bicellar formulations (Bartlett 1959). Hence, aliquots were removed from the bicelles suspension,
151 filtrate, or standard solution. The calibration curve was determined using standard solutions of
152 potassium phosphate monobasic (KH₂PO₄) in ultrapure water with concentrations ranging from
153 0.064 to 0.416 mM. The procedure is well described in our previous publications (Azzi et al.
154 2018b).

155 The incorporation rate (IR) of phospholipids was determined according to the following equation:

$$156 \quad \text{IR (\%)} = \frac{N_B - N_F}{N_I} \times 100$$

157 Where N_I is the initial number of moles of phospholipids and N_B and N_F are the total and free
158 number of moles of phospholipids determined in bicelle suspension, respectively.

159 ***2.4.5. Incorporation of nerolidol***

160

161 Ner was quantified in the bicellar formulations as previously described by Azzi et al. (2018a) using
162 an Agilent Technology 1200 series HPLC system. The mobile phase was a mixture of

163 methanol/water (75/25), the flow rate was set to 1 mL/min and the wavelength of the UV detector
164 was 212 nm. The calibration curve of Ner was determined using standard solutions of Ner in
165 methanol with concentrations ranging from 2.5 to 250 µg/mL. Thymol was used as an internal
166 standard at a concentration of 100 µg/mL in methanol. An aliquot (100 µL) of Ner standard
167 solution, filtrate obtained as described previously, or bicellar formulation with the adequate
168 dilution was added to 200 µL of methanol and 100 µL of thymol solution. The samples were then
169 sonicated for 10 min at 4 °C and centrifuged at 14,000 rpm for 30 min at 4 °C. An aliquot (20 µL)
170 of the supernatant was then analyzed through a reversed-phase C18 Agilent column (15 cm × 4.6
171 mm, 5 µm).

172 The encapsulation efficiency (EE) of Ner was determined according to the following equation:

173
$$EE (\%) = \frac{M_T - M_F}{M_T} \times 100$$

174 Where M_T and M_F are the total and free mass of Ner determined in the bicelles suspension,
175 respectively.

176 The molar percentage of Ner (%Ner) in bicelles was calculated as follows:

177
$$\%Ner = \frac{N_T - N_{Nf}}{N_B - N_F} \times 100$$

178 Where N_T and N_{Nf} are the total and free number of moles of Ner in the bicellar formulation,
179 respectively, and N_B and N_F are the total and free number of moles of phospholipids determined
180 in bicelle suspension, respectively.

181 **2.5. Effect of nerolidol on membrane fluidity**

182 **2.5.1. Fluorescence anisotropy measurements**

183 Steady state fluorescence polarization was used to determine the changes in bicelles fluidity using
184 a Cary Eclipse Fluorescence Spectrophotometer (Agilent Technologies). The fluorescent probe
185 DPH was dissolved in tetrahydrofuran at a concentration of 1 mg/mL. Bicellar suspensions were
186 incubated overnight in the dark at room temperature in presence of DPH at DPH:phospholipid
187 ratio of 1:500. The incubation allowed the intercalation of the probe into the lipid bilayer; the final
188 tetrahydrofuran concentration (< 0.01%) had no effect on the fluorescence anisotropy (Whiting et
189 al. 2000). The experiments were performed at 20, 25, 40, and 60 °C. The probe was excited at 360
190 nm with a manual polarizer accessory (Cary Eclipse Manual Polarizer, Agilent Technologies,
191 Malaysia) using vertically polarized light. The emission intensities were measured at 450 nm at
192 both parallel and perpendicular to the polarization vector of the exciting light. The Cary Eclipse
193 Bio Software, delivered from the spectrophotometer, gives the fluorescence anisotropy (R), which
194 is defined as:

195
$$R = \frac{I_{\parallel} - I_{\perp}}{I_{\parallel} + 2I_{\perp}},$$

196 Where I_{\parallel} and I_{\perp} are the fluorescence intensities of the light emitted with its polarization plane
197 parallel (\parallel) and perpendicular (\perp) to that of the exciting beam.

198 **2.5.2. Differential scanning calorimetry**

199

200 Calorimetric analysis of the bicellar formulations were performed using a DSC Q200 scanning
201 calorimeter (TA Instruments, France). An aliquot (30 μ L) of each formulation was placed in a
202 hermetically sealed standard aluminum DSC pans. The temperature was scanned at a rate of 1
203 °C/min over a range of 0 to 65 °C. The reference pan was filled with ultrapure water. The software
204 “TA processor” was then used to determine the phase transition temperature (T_m) from the

205 maximum of the recorded heat, the transition enthalpy (ΔH) from the area under the peak, the
206 respective pre-transition parameters (T_p and ΔH_p), and the temperature width at half peak height
207 ($\Delta T_{1/2}$). $\Delta T_{1/2}$ is inversely proportional to the cooperativity of the transition and thus will be
208 taken as a measure of the latter (El Maghraby et al. 2005).

209 **2.6. Statistical analysis**

210 Statistical analysis was performed using Student t-test, and P values equal to or less than 0.05
211 were considered to be significant.

212 **3. Results and discussion**

213 **3.1. Characterization of nerolidol-loaded bicelles**

214 ***3.1.1. Appearance, size, polydispersity index, zeta potential, and morphology***

215 Blank and nerolidol-loaded bicelles were prepared at 35 °C. At this temperature, the both lipids
216 DHPC and DMPC would be in the disordered fluid phase.

217 Blank bicelles and bicelles loading 1% Ner became transparent at room temperature after 18
218 freeze-thaw cycles. Formulations containing 2 and 5% Ner appeared turbid at room temperature
219 even at up to 40 freeze-thaw cycles. At higher Ner concentrations (10 and 25%), the formulations
220 had a milky appearance even after 40 cycles. Many essential oils including Ner are reported to
221 promote the enlargement of lipid particle size (Azzi et al. 2018a). Not surprisingly, the same effect
222 was maintained with bicelles. Rubio et al. (2011) have previously reported a milky appearance of
223 DPPC/DHPC bicellar system containing flufenamic acid (1% w/v) at 25 °C. In another study, the
224 same group (Rubio et al. 2010) has reported no change in the appearance of DPPC/DHPC and
225 DMPC/DHPC bicellar formulations following the addition of 1.16% (w/v) diclofenac. On the
226 other hand, Barbosa-Barros et al. (2008) reported a milky aspect of DMPC/DHPC bicellar

227 formulations containing ceramide (10 and 20%) at temperatures above the T_m of DMPC. At
228 temperatures below the T_m of DMPC, the appearance of the formulation was dependent on the
229 content of ceramide (Barbosa-Barros et al. 2008).

230 The size and the PDI values of bicelles were determined by DLS (Table 1) at a temperature below
231 the transition temperature (T_m) (19 ± 1 °C) and slightly higher than the T_m (25 ± 1 °C) of DMPC.
232 At 19 ± 1 °C, two populations were obtained for all bicellar formulations. Blank bicelles showed
233 a good homogeneity (PDI = 0.264). Around 95% of particles in the blank formulations had a size
234 around 42 nm (Table 1) which is in agreement with literature data (Barbosa-Barros et al. 2012),
235 while the minor population contained micrometric structures (Table 1). The formulation
236 containing Ner (1%) did not influence the size nor the homogeneity of the particles (Table 1).
237 Whereas, the addition of Ner at higher concentrations (2 to 25%) to the formulations increased
238 drastically the size of the particles of the major population for more than 10 folds and altered the
239 homogeneity of the formulations. At 25 °C, all formulations were highly polydispersed and the
240 major population in each formulation had a size greater than 300 nm. Our results agree with the
241 results previously obtained elsewhere (Barbosa-Barros et al. 2008) which reported an increase in
242 the particle size and heterogeneity at temperatures higher than the T_m of DMPC (30 and 40 °C). In
243 fact, temperatures above the T_m of the phospholipid promote the transfer of DHPC from the rim
244 to the DMPC bilayer domain, leading to the increase in the bicelles size (van Dam et al. 2006). On
245 the other hand, it has been reported that the change of the bicellar size is dependent on the location
246 of the incorporated agent. Drugs that intercalate between the long chain phospholipids such as
247 flufenamic acid produced an increase in bicelle size (Rubio et al. 2011). Similarly, increasing the
248 long chain- to short chain- phospholipid molar ratio increased the size of the bicelles due to the
249 enlargement of the planar bilayer (Vold and Prosser 1996). In contrast, drugs that join the rims like

250 diclofenac induced a decrease in bicelle size. Ner may localize into the planar bilayer of the bicelle
251 (Fig 1) between the acyl chains of DMPC, increasing their size. And, at high concentrations, Ner
252 may promote the formation of other lipid structures, like liposomes, as it will be subsequently
253 demonstrated by TEM analysis in this section.

254 On the other hand, blank bicelles had a zeta potential around -7 mV, which is close to the zeta
255 potential value of drug-free DMPC/DHPC bicelles reported by Yamada et al. (2016). The zeta
256 potential value was not greatly influenced by the addition of Ner at the different tested
257 concentrations (Table 1).

258 TEM analysis supports the results obtained by DLS. Indeed, bicelles prepared in the presence of
259 1% Ner appeared similar to blank bicelles (Fig 2 A-B). The stacks of bicelles that appear in Figures
260 2A and B may explain the micrometric population revealed by DLS analysis. The bicellar
261 formulation prepared in presence of Ner at concentrations higher than 1% led to the formation of
262 multilamellar sheets and/or liposomes (Fig 2 C-F). These structures had been observed elsewhere.
263 Fragments of multilamellar sheets and tubular structures, liposomes and elongated structures were
264 observed in the freeze fracture electron microscopy images of flufenamic acid-containing
265 DHPC/DPPC (2:1 molar ratio) bicelles formulation and TEM images of ceramid-containing
266 bicelles formulation (Barbosa-Barros et al. 2008; Rubio et al. 2011).

267 Ner-loaded liposomal formulations were previously prepared by Azzi et al. (2018a) and Ephrem
268 et al. (2019). The prepared suspensions had a phospholipid to Ner molar ratio of up to 10:1, particle
269 size higher than 131 nm, a milky appearance (Azzi et al. 2018a; Ephrem et al. 2019) and a low
270 homogeneity ($PdI > 0.48$) (Ephrem et al. 2019). Moreover, the addition of Ner-loaded liposomes
271 to fresh orange juice has altered the organoleptic property of the juice (Ephrem et al. 2019). This

272 problem could be overcome by the transparent appearance of bicellar formulations, thus
273 highlighting the importance of this system for the preparation of functional foods.

274 On the overall, the bicellar formulation prepared with Ner (1%) was retained for further
275 characterization because of the reliability of the bicellar structure that was confirmed through
276 particle size determination and morphological observation.

277 ***3.1.2. Encapsulation efficiency of nerolidol, incorporation rate of phospholipids and molar*** 278 ***percentage of nerolidol***

279 The bicelles preparation with Ner (1%) was characterized for the encapsulation efficiency (EE) of
280 Ner, molar percentage of Ner in bicelles (% Ner), and incorporation rate of phospholipids (IR) in
281 bicelles.

282 The quantification of phospholipids in the suspensions of blank bicelles showed that around 83.4
283 $\pm 1.2\%$ are incorporated in the bicelles and the incorporation rate increased in the presence of 1%
284 Ner (IR= $87.0 \pm 1.9\%$) (data not shown). On the other hand, the bicellar formulations prepared
285 with Ner 1% had an EE value of 100%. However, the molar percentage of Ner in bicelles was of
286 0.86%. The hydrophobicity of Ner and the length of its aliphatic chain (C_{12}) could explain the high
287 encapsulation efficiency value. Indeed, Ner ($C_{15}H_{26}O$) could be easily incorporated between the
288 DMPC molecules of acyl chains of 14 carbon atoms. Busch and Unruh (2011) previously reported
289 the intercalation of farnesol ($C_{15}H_{26}O$) between DMPC molecules inside the lipid bilayer by
290 aligning itself along the phospholipids molecules. On the other hand, it was proven that Ner may
291 completely penetrate the lipid bilayer (Mendanha and Alonso 2015).

292 **3.2. Effect of nerolidol on bicelles membrane fluidity**

293 ***3.2.1. Fluorescence anisotropy results***

294 The effect of Ner on the membrane fluidity of bicelles was investigated by steady-state
295 fluorescence anisotropy of DPH (Lakowicz 2006). The anisotropy values decreased when the
296 temperature increased from 20 to 40 °C at all the tested Ner concentrations, but then increased
297 slightly when the temperature increased between 40 and 60 °C (Fig 3). This may be due to the
298 occurrence of only one phase transition of the system at a temperature (23 °C) close to the T_m of
299 pure DMPC bilayers (Khatun et al. 2013). Similar observations had been made elsewhere on
300 formulations containing mixtures of phospholipids and gangliosides; above 40 °C, a plateau was
301 observed with anisotropy values slightly above or below those obtained at 40 °C for these
302 preparations (Khatun et al. 2013). The authors observed similar decrease of the anisotropy values
303 at temperatures ranging from 17 to 40 °C with DMPC/CHAPS (3-[(3-cholamidopropyl)
304 dimethylammonio]-1-propanesulfonate) bicelles. On the other hand, the presence of Ner increased
305 the membrane fluidity in a concentration dependent manner (Fig 3) at the tested temperatures. Yet,
306 a minimal change in the membrane fluidity was observed at Ner 1%. The increase of the membrane
307 fluidity in presence of Ner was expected since sesquiterpene alcohol has been previously reported
308 to increase the membrane fluidity of erythrocytes membranes (Mendanha et al. 2013) and plasma
309 membranes of parasites (Camargos et al. 2014).

310 ***3.2.2. Differential scanning calorimetry***

311 DSC is often used to study the thermodynamic properties of lipid bilayers. In fact, the
312 incorporation of an active agent can interfere with the packing of lipids thus changing the
313 thermodynamic parameters determined by DSC. The thermogram of DHPC exhibits no peak in
314 the studied temperature range (0 to 60 °C) (Rubio et al. 2011), thus the endotherms obtained most

315 likely arise from changes in the DMPC pre- and chain melting phase transitions at 9.3°C and 22.7°
316 C, respectively, in the presence of the increasing concentration of Ner.

317 In the absence of Ner, the bicellar system displayed a poor enthalpic pre-transition (9.3 ± 0.54 °C)
318 and a relatively sharp main transition (22.7 ± 0.40 °C) (Fig 4 and Table 2) which correspond
319 respectively to the transitions of DMPC acyl chains from $L_{\beta'}$ (gel phase) to $P_{\beta'}$ (ripple phase), and
320 from $P_{\beta'}$ to L_{α} (liquid crystalline phase) (Nagle 1980). The two peaks were previously reported by
321 Sasaki et al. (2007) (Sasaki et al. 2007) at around 12 and 23.6 °C, respectively for DMPC/DHPC
322 bicelles using DSC. On the other hand, the main phase transition enthalpy (ΔH , 9.21 ± 0.91 kJ/mol)
323 was significantly higher than that of the pre-transition (0.13 ± 0.07 kJ/mol) and was close to that
324 obtained by Sasaki et al. (2007) (1440 Cal/mol; 6.029 kJ/mol) (Sasaki et al. 2007). Small values
325 of $\Delta T_{1/2}$ and thus peak sharpness indicate the phase transition cooperativity ($1/\Delta T_{1/2}$) which is
326 determined by the purity of the lipid species being measured (Abboud et al. 2016). However, the
327 bicellar system showed a lower sharpness in the transition peak and a $\Delta T_{1/2}$ value of 3.95 ± 0.28
328 °C, which arises from the mixture of two lipids (DMPC/DHPC) with a corresponding decrease in
329 the chain melting phase transition cooperativity.

330 The pre-transition temperature decreases in presence of Ner and the peak is completely abolished
331 at Ner concentrations above 2% (Fig 4 and Table 2). Previous studies have explained the loss of
332 the pre-transition peak to the interaction of the added compound with the choline group of the
333 phospholipid (Abboud et al. 2016). Also, the chain melting phase transition temperature decreases
334 with the increasing Ner concentration, especially at Ner (25%) (Table 2). This could be explained
335 by the length of nerolidol chain (C12) compared to that of DMPC side chain (C14). In fact, sterols
336 with a chain length greater than the thickness of the bilayer increase the transition temperature of
337 DPPC bilayers while sterols with short side chains decrease the transition temperature (McMullen

338 et al. 1995). However, the main transition enthalpy is not significantly influenced by the presence
339 of 1, 2, and 5% Ner (Table 2). Whereas, at 25% Ner the ΔH increased (Table 2). On the other
340 hand, the presence of Ner increased the $\Delta T_{1/2}$ and led to the broadening of the main transition peak
341 (Fig 4 and Table 2).

342 The DPH fluorescence polarization measurements suggest that Ner is incorporated in the bicellar
343 bilayer leading to an increase of the membrane fluidity and this is supported by the decrease in the
344 chain melting phase transition cooperativity. Similarly, flufenamic acid increased the fluidity of
345 DPPC/DHPC bicelles (Rubio et al. 2011). DSC analysis showed that Ner produced a disorder in
346 the bicellar membrane. The smallest changes of thermodynamic parameters were obtained in the
347 presence of Ner (1%), which is in accordance with the results obtained by DLS, TEM, and DPH
348 anisotropy measurements

349 **Conclusion**

350 Ner was effectively incorporated in a bicellar system composed of DMPC and DHPC at a
351 phospholipids to Ner molar ratio of 100:1. The formulation exhibited similar appearance, particles
352 size range, PDI value, and morphology as the blank formulation. Moreover, it showed high EE
353 (100%) of Ner, and high IR ($87.0 \pm 1.9\%$) of phospholipids. At higher concentrations, Ner altered
354 the formulation characteristics. Finally, the fluidity of the bicelles bilayer increased in presence of
355 Ner, especially at Ner concentrations higher than 1%.

356 This study examines for the first time the possibility of the incorporation of an essential oil
357 component in a bicellar system. As a result, an optimized formulation was achieved which could
358 be a promising candidate to enhance the efficacy of Ner in food and pharmaceutical preparations.
359 Future trends could focus on the antimicrobial activity of Ner-loaded bicelles in culture media and
360 food matrices where other encapsulating systems made of lipids failed to preserve the organoleptic

361 properties of foods, especially juices. Also, the effect of the incorporation of other essential oil
362 components on the stability and characteristics of the bicellar system could be investigated.

363

364

365

366

367

368

369

370

371

372

373

374

375

376

377

378

379

380

381

382

383

384 **References**

- 385 Abboud R, Charcosset C, Greige-Gerges H (2016) Tetra- and Penta-Cyclic Triterpenes
386 Interaction with Lipid Bilayer Membrane: A Structural Comparative Study. *The Journal*
387 *of Membrane Biology* 249:327–338. <https://doi.org/10.1007/s00232-016-9871-8>
- 388 Azzi J, Auezova L, Danjou P-E, et al (2018a) First evaluation of drug-in-cyclodextrin-in-
389 liposomes as an encapsulating system for nerolidol. *Food Chemistry* 255:399–404.
390 <https://doi.org/10.1016/j.foodchem.2018.02.055>
- 391 Azzi J, Danjou P-E, Landy D, et al (2017) The effect of cyclodextrin complexation on the
392 solubility and photostability of nerolidol as pure compound and as main constituent of
393 cabreuva essential oil. *Beilstein Journal of Organic Chemistry* 13:835–844.
394 <https://doi.org/10.3762/bjoc.13.84>
- 395 Azzi J, Jraij A, Auezova L, et al (2018b) Novel findings for quercetin encapsulation and
396 preservation with cyclodextrins, liposomes, and drug-in-cyclodextrin-in-liposomes. *Food*
397 *Hydrocolloids* 81:328–340. <https://doi.org/10.1016/j.foodhyd.2018.03.006>
- 398 Barbosa-Barros L, De La Maza A, Walther P, et al (2008) Morphological effects of ceramide on
399 DMPC/DHPC bicelles. *Journal of Microscopy* 230:16–26. [https://doi.org/10.1111/j.1365-](https://doi.org/10.1111/j.1365-2818.2008.01950.x)
400 [2818.2008.01950.x](https://doi.org/10.1111/j.1365-2818.2008.01950.x)
- 401 Barbosa-Barros L, Rodríguez G, Barba C, et al (2012) Bicelles: Lipid Nanostructured Platforms
402 with Potential Dermal Applications. *Small* 8:807–818.
403 <https://doi.org/10.1002/smll.201101545>

404 Bartlett GR (1959) Phosphorus assay in column chromatography. *Journal of Biological*
405 *Chemistry* 234:466–468

406 Busch S, Unruh T (2011) The influence of additives on the nanoscopic dynamics of the
407 phospholipid dimyristoylphosphatidylcholine. *Biochimica et Biophysica Acta (BBA) -*
408 *Biomembranes* 1808:199–208. <https://doi.org/10.1016/j.bbamem.2010.10.012>

409 Camargos HS, Moreira RA, Mendanha SA, et al (2014) Terpenes Increase the Lipid Dynamics
410 in the Leishmania Plasma Membrane at Concentrations Similar to Their IC50 Values.
411 *PLoS ONE* 9:e104429. <https://doi.org/10.1371/journal.pone.0104429>

412 Chan W-K, Tan LT-H, Chan K-G, et al (2016) Nerolidol: A Sesquiterpene Alcohol with Multi-
413 Faceted Pharmacological and Biological Activities. *Molecules* 21:529.
414 <https://doi.org/10.3390/molecules21050529>

415 Chen J, Lu W-L, Gu W, et al (2014) Drug-in-cyclodextrin-in-liposomes: a promising delivery
416 system for hydrophobic drugs. *Expert Opinion on Drug Delivery* 11:565–577.
417 <https://doi.org/10.1517/17425247.2014.884557>

418 Dürr UHN, Gildenberg M, Ramamoorthy A (2012) The Magic of Bicelles Lights Up Membrane
419 Protein Structure. *Chem Rev* 112:6054–6074. <https://doi.org/10.1021/cr300061w>

420 El Maghraby GMM, Williams AC, Barry BW (2005) Drug interaction and location in liposomes:
421 correlation with polar surface areas. *Int J Pharm* 292:179–185.
422 <https://doi.org/10.1016/j.ijpharm.2004.11.037>

423 Ephrem E, Najjar A, Charcosset C, Greige-Gerges H (2019) Use of free and encapsulated
424 nerolidol to inhibit the survival of *Lactobacillus fermentum* in fresh orange juice. *Food*
425 *and Chemical Toxicology* 133:110795. <https://doi.org/10.1016/j.fct.2019.110795>

426 Khatun UL, Gayen A, Mukhopadhyay C (2013) Gangliosides containing different numbers of
427 sialic acids affect the morphology and structural organization of isotropic phospholipid
428 bicelles. *Chemistry and Physics of Lipids* 170–171:8–18.
429 <https://doi.org/10.1016/j.chemphyslip.2013.02.009>

430 Lakowicz JR (2006) *Principles of fluorescence spectroscopy*, Third. Springer, New York

431 Lin L, Wang X, Guo Y, et al (2016) Hybrid bicelles as a pH-sensitive nanocarrier for
432 hydrophobic drug delivery. *RSC Adv* 6:79811–79821.
433 <https://doi.org/10.1039/C6RA18112K>

434 Marsanasco M, Piotrkowski B, Calabró V, et al (2015) Bioactive constituents in liposomes
435 incorporated in orange juice as new functional food: thermal stability, rheological and
436 organoleptic properties. *Journal of Food Science and Technology* 52:7828–7838.
437 <https://doi.org/10.1007/s13197-015-1924-y>

438 McMullen TP, Vilchère C, McElhaney RN, Bittman R (1995) Differential scanning calorimetric
439 study of the effect of sterol side chain length and structure on
440 dipalmitoylphosphatidylcholine thermotropic phase behavior. *Biophysical Journal*
441 69:169–176. [https://doi.org/10.1016/S0006-3495\(95\)79887-3](https://doi.org/10.1016/S0006-3495(95)79887-3)

442 Mendanha SA, Alonso A (2015) Effects of terpenes on fluidity and lipid extraction in
443 phospholipid membranes. *Biophysical Chemistry* 198:45–54.
444 <https://doi.org/10.1016/j.bpc.2015.02.001>

445 Mendanha SA, Moura SS, Anjos JLV, et al (2013) Toxicity of terpenes on fibroblast cells
446 compared to their hemolytic potential and increase in erythrocyte membrane fluidity.
447 *Toxicology in Vitro* 27:323–329. <https://doi.org/10.1016/j.tiv.2012.08.022>

448 Miranda JC de, Martins TEA, Veiga F, Ferraz HG (2011) Cyclodextrins and ternary complexes:
449 technology to improve solubility of poorly soluble drugs. *Brazilian Journal of*
450 *Pharmaceutical Sciences* 47:665–681. [https://doi.org/10.1590/S1984-](https://doi.org/10.1590/S1984-82502011000400003)
451 [82502011000400003](https://doi.org/10.1590/S1984-82502011000400003)

452 Moreira da Silva A (2009) Cyclodextrins as food additives and ingredients: Nutraceutical
453 applications. In 9th food chemistry meeting. Portugal.

454 Nagle JF (1980) Theory of the Main Lipid Bilayer Phase Transition. *Annual Review of Physical*
455 *Chemistry* 31:157–196. <https://doi.org/10.1146/annurev.pc.31.100180.001105>

456 Rajewski RA, Stella VJ (1996) Pharmaceutical applications of cyclodextrins. 2. In vivo drug
457 delivery. *J Pharm Sci* 85:1142–1169. <https://doi.org/10.1021/js960075u>

458 Rubio L, Alonso C, Rodríguez G, et al (2010) Bicellar systems for in vitro percutaneous
459 absorption of diclofenac. *International Journal of Pharmaceutics* 386:108–113.
460 <https://doi.org/10.1016/j.ijpharm.2009.11.004>

461 Rubio L, Rodríguez G, Alonso C, et al (2011) Structural effects of flufenamic acid in
462 DPPC/DHPC bicellar systems. *Soft Matter* 7:8488. <https://doi.org/10.1039/c1sm05692a>

463 Sasaki R, Sasaki H, Fukuzawa S, et al (2007) Thermal Analyses of Phospholipid Mixtures by
464 Differential Scanning Calorimetry and Effect of Doping with a Bolaform Amphiphile.
465 *Bulletin of the Chemical Society of Japan* 80:1208–1216.
466 <https://doi.org/10.1246/bcsj.80.1208>

467 van Dam L, Karlsson G, Edwards K (2006) Morphology of Magnetically Aligning
468 DMPC/DHPC Aggregates Perforated Sheets, Not Disks. *Langmuir* 22:3280–3285.
469 <https://doi.org/10.1021/la052988m>

470 Visscher I, Stuart MCA, Engberts JBFN (2006) The influence of phenyl and phenoxy
471 modification in the hydrophobic tails of di-n-alkyl phosphate amphiphiles on aggregate
472 morphology. *Org Biomol Chem* 4:707–712. <https://doi.org/10.1039/B514285G>

473 Vold RR, Prosser RS (1996) Magnetically Oriented Phospholipid Bilayered Micelles for
474 Structural Studies of Polypeptides. Does the Ideal Bicelle Exist? *Journal of Magnetic*
475 *Resonance, Series B* 113:267–271. <https://doi.org/10.1006/jmrb.1996.0187>

476 Whiting KP, Restall CJ, Brain PF (2000) Steroid hormone-induced effects on membrane fluidity
477 and their potential roles in non-genomic mechanisms. *Life Sci* 67:743–757

478
479
480
481
482

483 **Figure captions**

484 **Fig.1** A schematic representation of an ideal bicelle

485 **Fig.2** TEM images of bicelles containing A) 0, B) 1, C) 2, D) 5, E) 10, and F) 25% Ner

486 **Fig.3** DPH anisotropy values for bicelles with or without Ner at phospholipid to Ner molar ratios
487 of 100:1, 50:1, 20:1, 10:1, and 4:1 at 20, 25, 40, and 60 °C

488 **Fig.4** DSC scans of blank bicelles and Ner-loaded bicelles at phospholipid to Ner molar ratios of
489 100:0, 100:1, 50:1, 20:1, 10:1, and 4:1

490

491

492

493

494

495

496

497

498

499

500

501

502

503 **Table 1: Size, polydispersity index, and zeta potential of bicellar formulations with and**
 504 **without nerolidol.**

19 ± 1 °C						
Ner %	Population 1		Population 2		PdI	Zeta potential (mV)
	%	Size (nm)	%	Size (nm)		
0	95.2 ± 4.6	42.2 ± 4.8	5.8 ± 4.9	3607 ± 1869	0.26 ± 0.04	-6.9 ± 1.0
1	96.8 ± 4.4	45.2 ± 5.5	4.9 ± 2.4	3715 ± 659*	0.19 ± 0.07	-9.6 ± 1.9
2	36.6 ± 2.4	41.1 ± 5.5	63.4 ± 2.4	624 ± 205*	0.69 ± 0.09*	-9.6 ± 3.5
5	40.2 ± 9.4	46.6 ± 7.1	59.8 ± 12.0	404 ± 172*	0.74 ± 0.20*	-6.1 ± 0.0
10	11.0 ± 3.4	128.5 ± 25.4*	89.0 ± 6.3	1532 ± 70*	0.73 ± 0.09*	-6.7 ± 0.5
25	88.5 ± 11.6	434.5 ± 2.5*	23.1 ± 12.2	2561 ± 703*	0.44 ± 0.01*	-12.2 ± 0.5
25 ± 1 °C						
Ner %	Population 1		Population 2		PdI	Zeta potential (mV)
	%	Size (nm)	%	Size (nm)		
0	45.8 ± 23.3	48.7 ± 16.9	54.2 ± 23.3	515 ± 278	0.54 ± 0.19	-12.7 ± 6.3
1	42.7 ± 13.1	38.4 ± 7.85	56.3 ± 14.2	322 ± 68	0.53 ± 0.14	-14.1 ± 5.6
2	13.8 ± 4.3	170.9 ± 101.5	81.9 ± 8.7	1161 ± 470*	0.74 ± 0.26	-18.3 ± 5.2
5	9.8 ± 5.4	183.6 ± 33.8	70.5 ± 30.4	906 ± 358	0.82 ± 0.15	-10.9 ± 0.4
10	3.9 ± 3.8	61.9 ± 56.1*	96.1 ± 3.8	560 ± 119	0.28 ± 0.03*	-8.8 ± 0.8
25	25.0 ± 5.1	148.4 ± 13.6*	85.0 ± 15.1	494 ± 78	0.61 ± 0.17	-12.2 ± 2

505 * *P* values equal to or less than 0.05

506

507

508

509

510

511

512

513

514 **Table 2: Parameters with increasing Ner concentration in DMPC/DHPC (2:1 molar ratio)**
515 **bicelles.**

%Ner	T _p (°C)	ΔH _p (Kj/mol)	T _m (°C)	ΔH (Kj/mol)	ΔT _{1/2} (°C)
0	9.30 ± 0.54	0.13 ± 0.07	22.70 ± 0.40	9.21 ± 0.91	3.95 ± 0.28
1	7.74 ± 0.14	0.12 ± 0.01	22.30 ± 0.11	8.69 ± 0.61	4.32 ± 0.15
2	4.96 ± 0.78	0.16 ± 0.05	21.40 ± 0.02	9.91 ± 0.04	5.06 ± 0.11
5	-	-	20.50 ± 0.11	9.40 ± 0.36	6.03 ± 0.41
25	-	-	13.50 ± 0.02	11.67 ± 0.2	8.51 ± 0.18

516

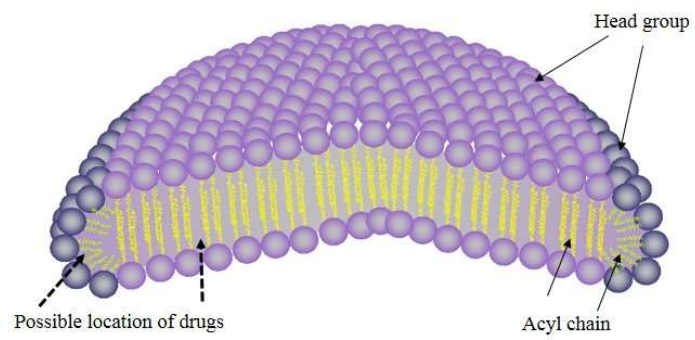
517

518

519 Figure 1

520

521



522

523

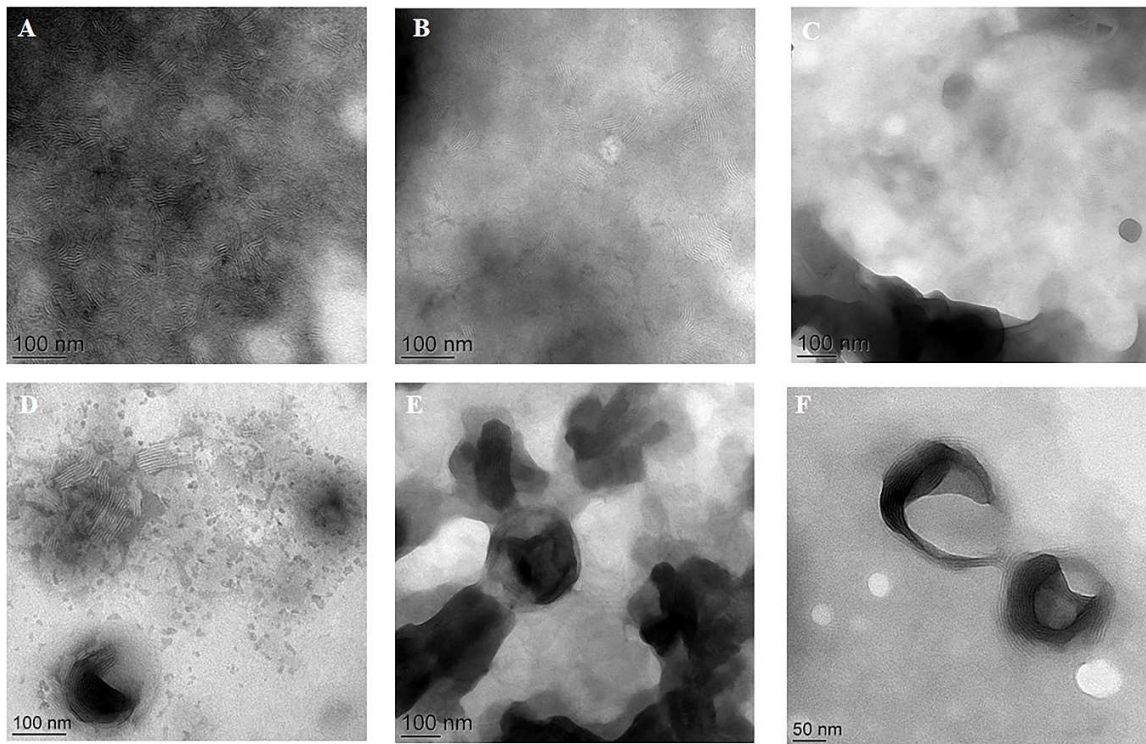
524

525

526

527 Figure 2

528



529

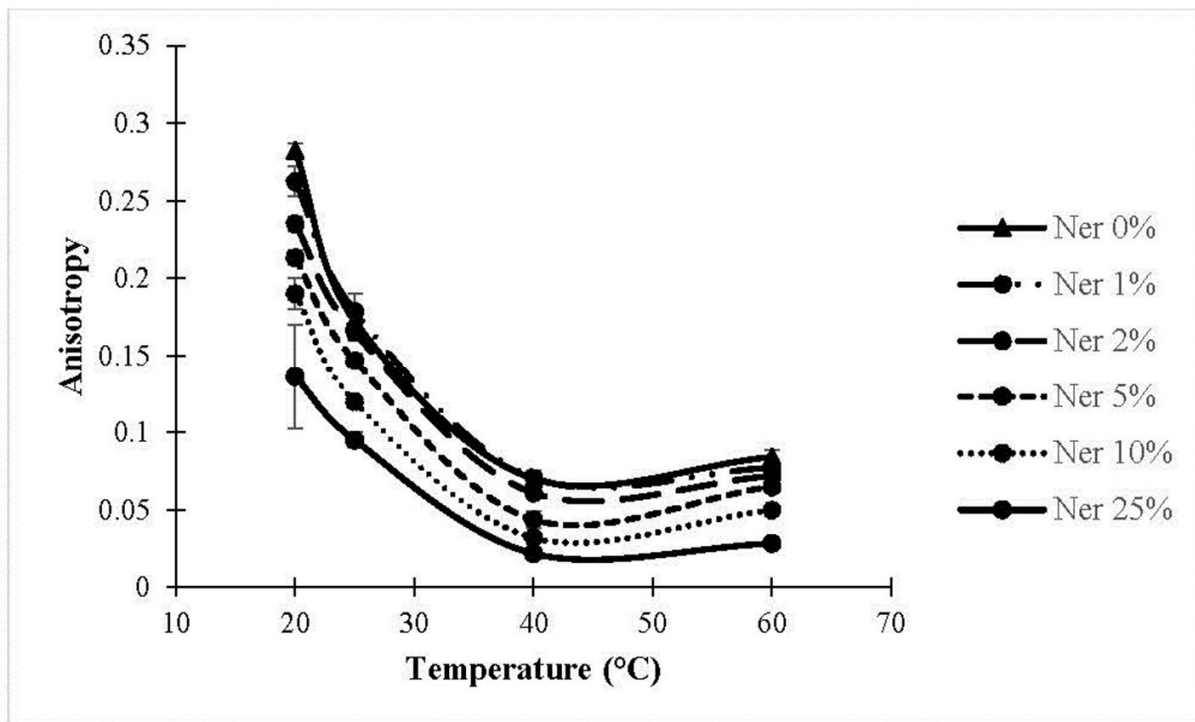
530

531

532

533 Figure 3

534



535

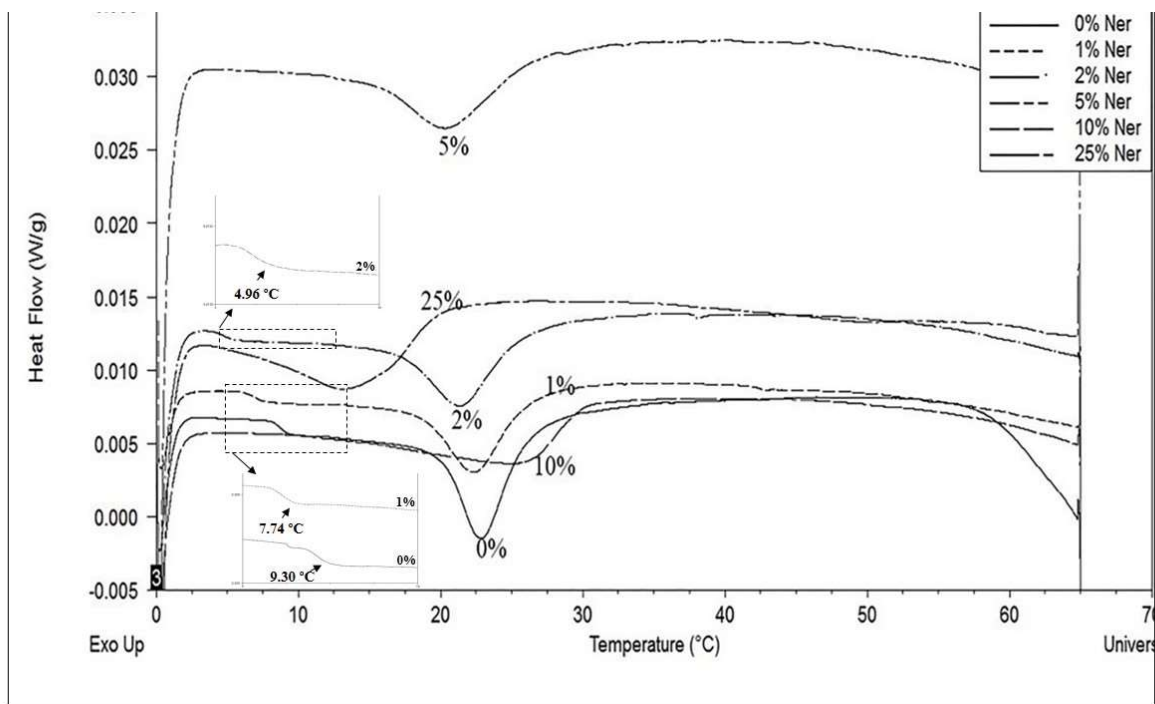
536

537

538

539 Figure 4

540



541